Electrical Interconnection with a Smart ACA Composed of Fluxing Polymer and Solder Powder

Yong-Sung Eom, Keon-Soo Jang, Jong-Tae Moon, and Jae-Do Nam

The interconnection mechanisms of a smart anisotropic conductive adhesive (ACA) during processing have been characterized. For an understanding of chemorheological mechanisms between the fluxing polymer and solder powder, a thermal analysis as well as solder wetting and coalescence experiments were conducted. The compatibility between the viscosity of the fluxing polymer and melting temperature of solder was characterized to optimize the processing cycle. A fluxing agent was also used to remove the oxide layer performed on the surface of the solder. Based on these chemorheological phenomena of the fluxing polymer and solder, an optimum polymer system and its processing cycle were designed for high performance and reliability in an electrical interconnection system. In the present research, a bonding mechanism of the smart ACA with a polymer spacer ball to control the gap between both substrates is newly proposed and investigated. The solder powder was used as a conductive material instead of polymer-based spherical conductive particles in a conventional anisotropic conductive film.

Keywords: Smart ACA, anisotropic conductive adhesive, fluxing polymer, solder powder, electrical interconnection.

Manuscript received July 13, 2009; revised Oct. 22, 2009; accepted Dec. 4, 2009

This work was supported by the IT R&D program of MIC/IITA, Rep. of Korea (2006-S-056-01, Anisotropic Conductive material for IT Components).

Yong-Sung Eom (phone: 82 42 860 5547, email: yseom@eti.re.kr) and Jong-Tae Moon (email: jtmoon@eti.re.kr) are with the Convergence Components & Materials Research Laboratory, ETRI, Daejeon, Rep. of Korea

Keon-Soo Jang (email: pitcherboy@skku.edu) and Jae-Do Nam (email: jdnam@skku.edu) are with the Department of Polymer Science and Engineering, Sungkyunkwan University, Suwon, Rep. of Korea

doi:10.4218/etrij.10.0109.0400

I. Introduction

With the need of a more reliable and stable electrical interconnection for highly integrated microelectronic packaging, many kinds of interconnection materials such as a solder ball using a C4 process and a conventional anisotropic conductive film (ACF) with a metal coated polymer ball, have been markedly developed [1]-[4]. As a first-generation electrical interconnection, C4 technology is widely used in surface mounting technology (SMT) with a flux application. After the soldering process, the residual flux is cleaned and an underfill process is then conducted to obtain highly reliable performance if required for portable communication devices or consumer electronics. This metallurgical bonding with the underfill process has been the main interconnection method for flip-chip bonding since its development by IBM more than 40 years ago. However, this conventional soldering process basically requires a high processing temperature and a long processing time. It also has environmental considerations due to the use of fluxes and cleaning agents. For these reasons, a conventional ACF with a polymer particle covered by a conductive metal layer was developed as a second-generation microelectronic interconnection method [5]. The conventional ACF has offered several advantages, such as a relatively low processing temperature, high adhesion strength, short processing time, and elimination of flux and cleaning processes. In principle, the electrical conduction of a conventional ACF is achieved by the mechanical contact of a conductive metal layer deposited on the polymer particle. This could be a handicap for good electrical and thermal conductivity and packaging reliability for active device applications. In the meantime, a new electrical interconnection method as a third-generation electronic material was proposed by P. Savolainen and others to

satisfy such packaging issues as a no-cleaning process of the flux material, high electrical and thermal conductivity, a reduction of processing costs, good adhesion strength, and high reliability [6], [7]. Their new anisotropic conductive adhesive (ACA) is composed of a polymer resin that functions as a flux material and a solder powder of about 5% in volume. Kim and others have recently researched a conductive adhesive using fusible solder fillers [8], [9]. They have carefully observed and analyzed the curing behavior of polymer resin, solder coalescence, and the wetting phenomenon, as well as the electrical performance according to the several kinds of polymer binders. Many researchers have investigated no-flow underfill materials with an oxide elimination function performed on the solder surface for flip-chip applications [10]-[12]. A solder ball of about 0.7 mm in diameter with a relatively small surface area compared to the solder powder was used for all of these experiments. S. Shi and others extensively studied the effects of a fluxing agent mixed with a polymer resin and its reliability [11]. They observed that the underfill material mixed with the fluxing agent did not show remarkable effects regarding CTE α_1, storage modulus, moisture absorption, or corrosion potential.

In other previous studies [13], [14], the fundamental processing mechanism of a new ACA as a third-generation electrical interconnection material, named smart ACA, was characterized by way of chemorheological and electrical performances. The smart ACA was designed to be able to conduct SMT and underfill processes at the same time. The present research aims to design and evaluate an optimum processing condition for a smart ACA material based on a new resin system with a fluxing performance, as well as a gap control technology between pads in the through-thickness direction using a polymer spacer.

II. Materials and Experimental

1. Materials

The fluxing polymer is composed of five components, a base resin, curing agent, catalyst to control the chemical reaction rate, polymer ball as a spacer to control the gap between the upper and bottom substrates, and a fluxing agent to remove the oxide layer performed on the surface of the solder powder. The solder powder used for the smart ACA is Sn/58Bi with an average diameter of 45 μm, as shown in Fig. 1. The volume ratio between solder powder and fluxing polymer is 30:70. The chemical and metal components were purchased from commercial sources and used as received.

2. Experiment

In order to understand the chemorheological reaction

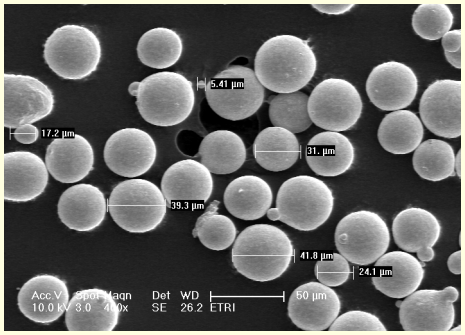

Fig. 1. SEM photograph of Sn/58Bi with an average diameter of 45 μm.

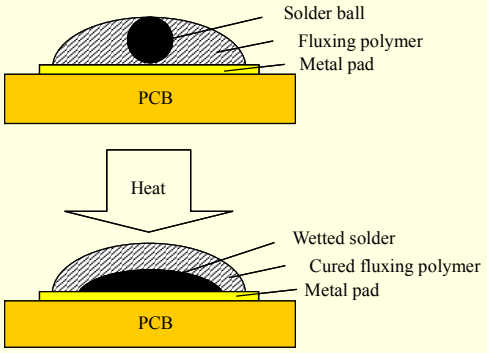

Fig. 2. Measurement method for the solder wetting angle with a diameter of 0.76 mm on Au and Cu pads.

mechanism of the fluxing polymer and smart ACA, differential scanning calorimetry (DSC) and a dynamic mechanical analyzer (DMA) are used with a heating rate of 10°C/min. For the DMA experiment, a torsional parallel plate with a diameter of 20 mm was used within a torsional frequency of 1 Hz and a controlled stress of 100 Pa. Figure 2 shows the measurement method for the wetting angle of an Sn/58Bi solder ball with a diameter of 0.76 mm on Au and Cu metal pads. If the diameter of the solder powder is decreased, the concentration of the fluxing agent should be theoretically increased because the surface area of the solder powder is in inverse proportion with its diameter when the total volume of the solder powder is constant. For the measurement of the solder wetting angle, the temperature on a hot plate is increased up to 180°C with a heating rate of 43°C/min.

Figures 3 and 4 show a schematic of a flip-chip bonding procedure and its process cycle for the smart ACA, respectively. After an alignment step for a flip-chip bonding process corresponding to time = 0 as shown in Fig. 4, the smart ACA composed of fluxing polymer, Sn/58Bi solder powder with a diameter of 45 μm, and a spacer with a diameter of about 50 μm is placed between the upper and bottom PCBs, as

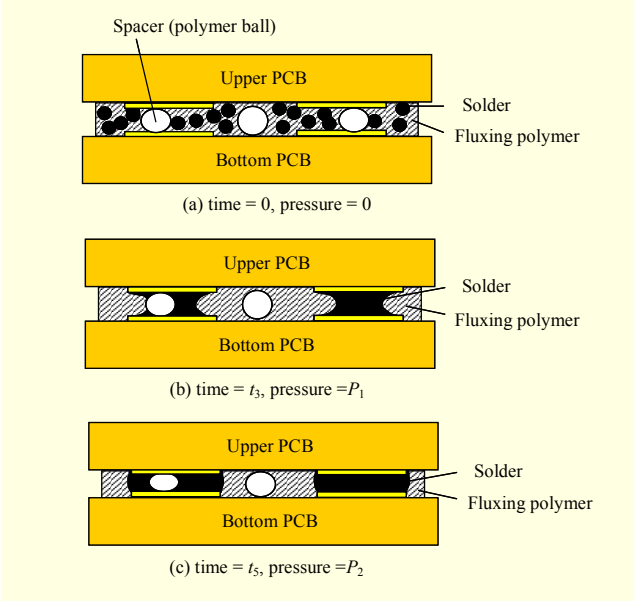

Fig. 3. Schematics of the flip-chip bonding procedure with the smart ACA.

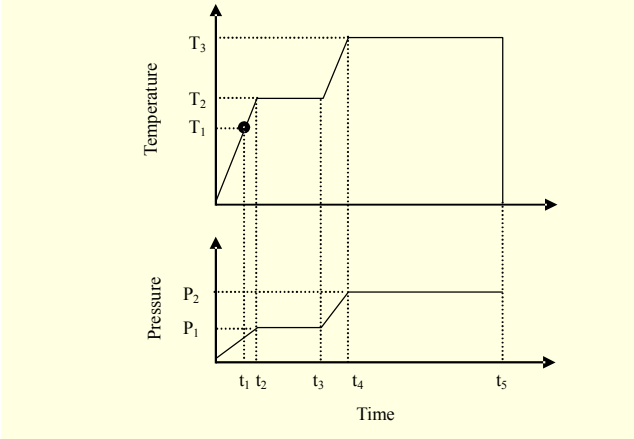

Fig. 4. Processing cycle of flip-chip bonding for the smart ACA.

shown in Fig. 3(a). With an increase of processing temperature, the solder powder begins to melt, coalesce, and become wetted on the pads within the liquid state of the fluxing polymer when the temperature passes the melting temperature of the solder (T_1). When the temperature reaches T_2, it is held and maintained until time t_3 with applied pressure P_1, as shown in Fig. 3(b). At time t_3, the gap between the upper and bottom PCBs is determined by the balance between applied pressure P_1 and the compression force of the polymer spacer. In this equilibrium state, the shape of the melted solder between the upper and bottom metal pads will be concave within the liquid state of the fluxing polymer, as shown in Fig. 3(b). However, isolated solder powder that is not coalesced and wetted on both metal pads can possibly exist if the space between the pads is large enough in the horizontal direction. Afterward, the applied

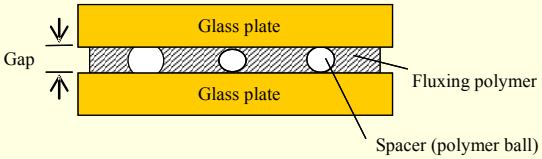

Fig. 5. Experiment to obtain a gap between the glass plates according to the applied pressure.

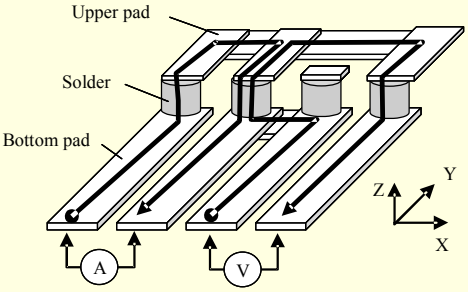

Fig. 6. Schematic of the experimental setup to measure the electrical resistance using a 4-point probe.

pressure is increased up to P_2 in order to obtain a more stable shape of the solder interconnection between the metal pads, and the process temperature reaches T_3 and keeps to time t_5 in order to obtain a fully cured state of the fluxing polymer, as shown in Fig. 4. Finally, the solder between the metal pads shows the convex shape shown in Fig. 3(c), and the gap between both metal pads is decided based on the equilibrium between applied pressure P_2 and the compression force of the polymer spacer. For the flip-chip bonding process, the upper and bottom PCBs with a pad dimension of 0.2 mm × 3 mm and a 0.4 mm pitch were prepared. The metal pads were electroplated using 5 μm Ni and 0.6 μm Au.

In order to determine the optimum applied pressure during the given temperature cycle, the gap variation according to the applied pressure was measured by the experimental method shown in Fig. 5. The fluxing polymer mixed with the polymer spacer is placed between the glass plates and is processed under the given temperature cycle and several applied pressures. After processing, the gap was measured as a function of the different spacer amounts and applied pressures. In summary, SMT and the underfill processes are simultaneously conducted by the smart ACA without the cleaning process after SMT. In order to prevent a phenomenon of a solder bridging between neighboring pads in a horizontal axis, the smart ACA should be precisely designed considering the following items: an areal ratio between a pad and a space in between adjacent pads, a volumetric ratio between the solder and the fluxing polymer, a volume ratio between the spacer with polymer ball and the fluxing polymer, the initial thickness of the smart ACA

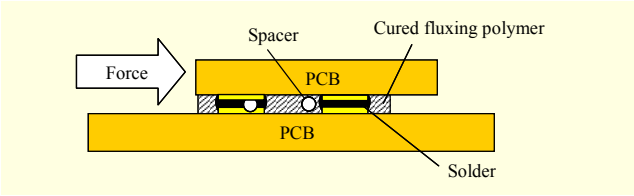

Fig. 7. Schematic of the shear test with the smart ACA material.

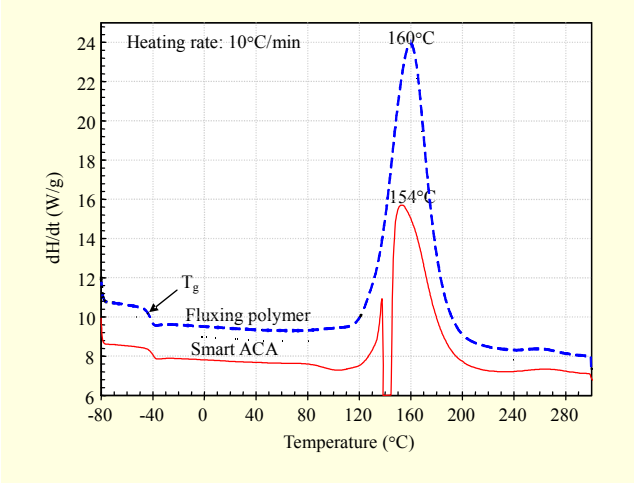

Fig. 8. Dynamic DSC thermograms of the fluxing polymer and smart ACA materials with a heating rate of 10°C/min.

in Fig. 3 (a), and the applied pressure during a bonding process.

Figure 6 shows the experimental setup of a 4-point probe method used to measure the electrical resistance of a solder interconnection with the smart ACA material. The voltage is measured from the two right channels when a direct current is applied to the two left channels. From the measured voltage and current, the electrical resistance is easily obtained. After a flip-chip bonding process, the shear strength of the fluxing polymer was measured using the shear test.

III. Results and Discussion

Figure 8 shows the dynamic DSC results of the fluxing polymer and smart ACA with a heating rate of 10°C/min. The glass transition temperature, T_g, of both uncured materials was measured at −40°C, and it was observed that the initial reaction temperature of the smart ACA was slightly earlier than the fluxing polymer at around 120°C.

With increasing temperature, the smart ACA shows a melting phenomenon of solder at around 140°C, and the peak temperatures of the chemical reaction of the fluxing polymer and smart ACA were 160°C and 154°C, respectively. In other words, the temperatures related to polymerization, such as the beginning temperature of a chemical reaction and peak temperature, are influenced by the presence of the solder

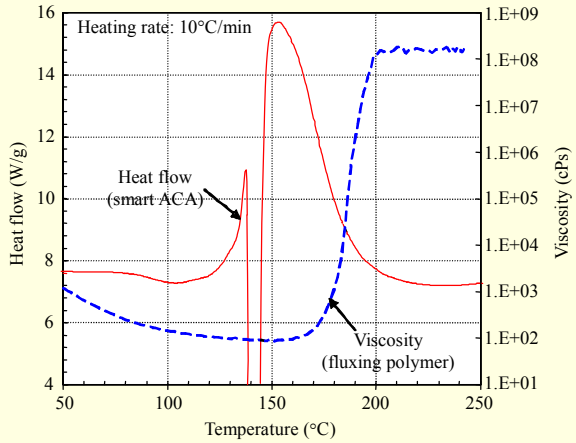

Fig. 9. Comparison of heat flow from DSC thermograms with a smart ACA, and viscosity from the DMA with the fluxing polymer.

powder, while the glass transition temperature of uncured materials, which is not related to the chemical reaction, is not changed by the solder powder.

It could be inferred that this phenomenon was caused by the catalytic effect of Sn/Bi solder powder for the polymerization. Figure 9 shows a comparison of the heat flow from DSC with the smart ACA, and the viscosity of the fluxing polymer. If the catalytic effect of solder powder is considered, the viscosity curve of the smart ACA should be linearly shifted as much as 6°C toward the lower temperature direction. As shown in Fig. 9, the viscosity of the fluxing polymer around the melting temperature of solder powder indicates about 200 cPs, which is sufficiently low for solder coalescence and wetting. Therefore, it is clear that the given fluxing polymer system is optimally designed from the harmonization between solder melting and polymerization. If the heating rate of the smart ACA is increased during processing, the peak temperature of the chemical reaction is increased while the melting temperature of solder is almost constant. In order to obtain a conversion of the smart ACA after the curing process, the relationship between conversion and glass transition temperature is expressed using the modified Dibeneditto equation (1) and Fig. 10 [15].

$$T_g = T_{g0} + \frac{(T_{g\infty} - T_{g0})\lambda\alpha}{1-(1-\lambda)\alpha}, \quad (1)$$

where T_{g0} is the T_g of the uncured polymer, $T_{g\infty}$ is the T_g of the fully cured polymer, α is the conversion, and λ is the polymer structure dependent parameter. After the given curing process, the glass transition temperature and conversion were measured using a dynamic DSC with a heating rate of 10°C/min. In Fig. 10, there is good agreement between the measured and predicted data when T_{g0} is −40°C, $T_{g\infty}$ is 138°C, and λ is 0.35. Therefore, the conversion after processing can be easily

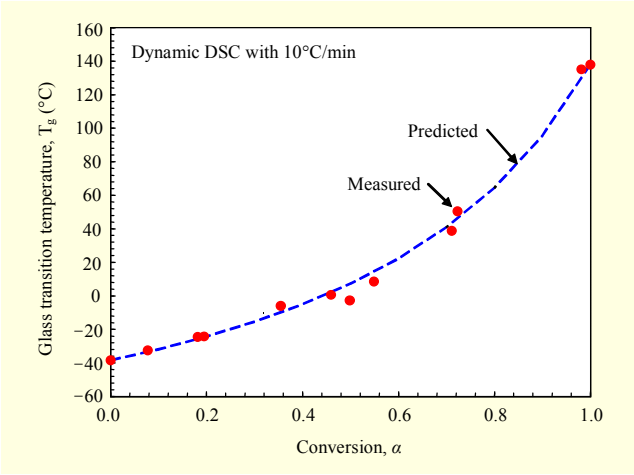

Fig. 10. Comparison of the measured and predicted glass transition temperature as a function of the conversion.

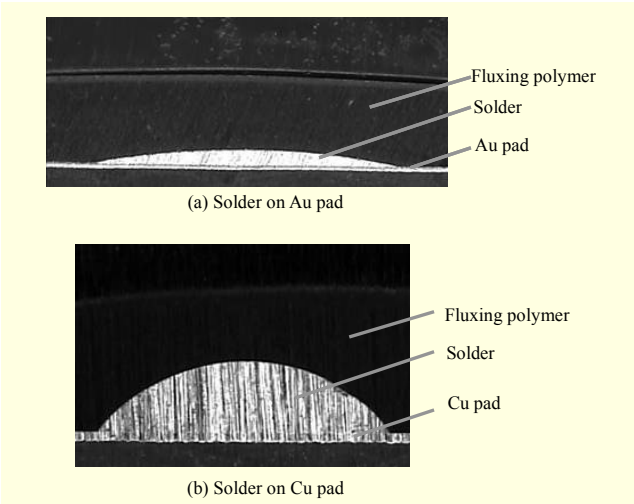

Fig. 11. Cross-sectional photographs of wetted solder balls with a diameter of 0.76 mm on Au and Cu pads.

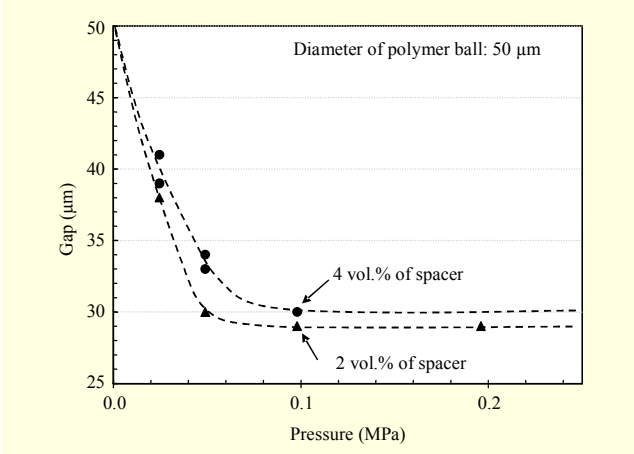

Fig. 12. Measured gap between glass plates with different spacer concentration according to the applied process pressure.

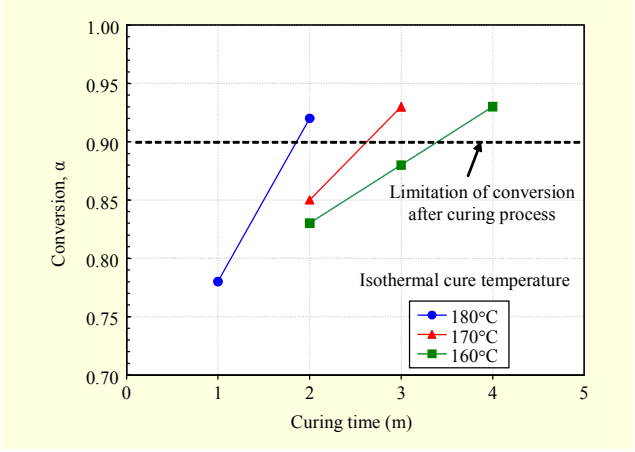

Fig. 13. Conversion as a function of curing time and temperature.

calculated by (1) as a function of the measured glass transition temperature.

The solder balls with a diameter of 0.76 mm in the fluxing polymer on the Au and Cu pads were heated. After processing, the wetted solder was covered by the cured fluxing polymer as shown in Fig. 11. The diameters and angles of the wetted solder on the Au and Cu pads were 1.92 and 1.25 mm, and 9.4 and 48.8 degrees, respectively. From this measurement, it is clearly identified that the oxide layer performed on the surface of the solder powder, as well as on the Au and Cu pad surfaces, is clearly removed.

In order to decide the processing pressure, the gap determined by the polymer spacer with an average diameter of 50 μm placed between the glass plates was measured after the flip-chip bonding process. Figure 12 shows a gap with spacers of 2% and 4% in weight in the fluxing polymer as a function of applied pressure. With the increase of applied pressure, the gap is rapidly decreased to 30 μm with 0.05 MPa pressure, and keeps a constant value of about 30 μm until 0.2 MPa pressure for both spacer volume percentages as shown in Fig. 12. From the measurement results in Fig. 12, it is proved that the applied pressure of 0.1 MPa and spacer of 2% in weight were optimum conditions for the stable flip-chip bonding process because a lower spacer percentage is much better to obtain a large solder wetting area on a pad.

Figure 13 shows the conversion of a fluxing polymer as a function of isothermal curing temperature and time. The experimental results show that the conversion of the fluxing polymer is higher than 0.9 if the curing time is longer than about 2 min at 180°C or 4 min at 160°C. From an industrial point of view, polymer material with a conversion of 0.9 is considered fully cured in its thermal and mechanical properties. If the processing time is important for a smart ACA application, a processing temperature of 180°C will be chosen. However, if the smart ACA material is processed with a peripheral device,

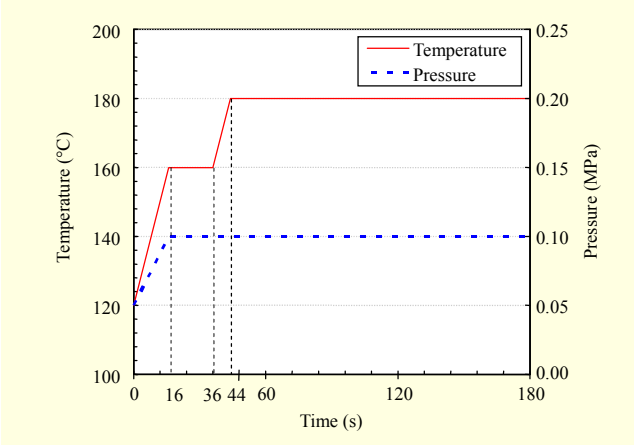

Fig. 14. Optimum processing cycle for flip-chip bonding with a smart ACA.

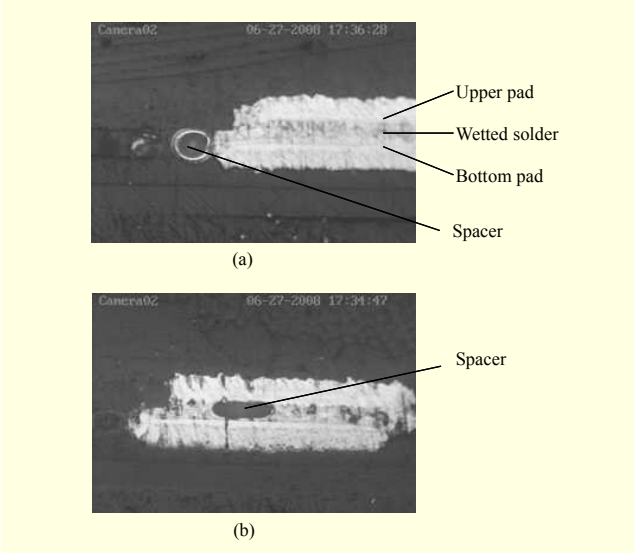

Fig. 15. Optical microscope photograph of a cross-sectional view of bonded PCBs after the flip-chip bonding process.

such as a polymer lens with a lower melting point than 180°C, a processing temperature of 160°C should be used even though the processing time is longer. Based on the experimental results shown in Figs. 12 and 13, the optimum processing cycle for a flip-chip bonding condition was carefully designed for the smart ACA, as shown in Fig. 14. With an increase of processing time, the temperature and pressure are increased to 160°C, which is higher than the melting point of solder, and 0.1 MPa, respectively. The temperature is then maintained for 10 sec and increased to 180°C, and maintained again for 136 sec.

As shown in Fig. 15, the solder powder was coalesced and wetted between the upper and bottom pads with a thickness of about 19 μm. Some of the polymer spacer was placed between the pads in the horizontal direction in Fig. 15(a), or in the through-thickness direction in Fig. 15 (b). The thickness of the

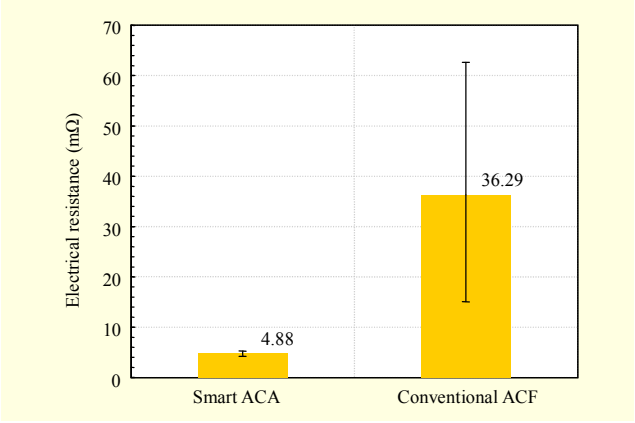

Fig. 16. Comparison of the electrical resistance between the smart ACA and a conventional ACF.

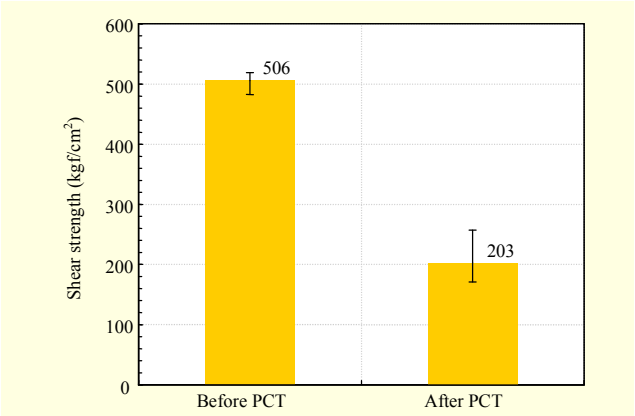

Fig. 17. Comparison of shear strength before and after PCT of the smart ACA.

solder was determined using a spacer with the compressed shape shown in Fig. 15(b) because the shape of the spacer between the pads in the horizontal direction appears almost as a circle without a compression force as shown in Fig. 15(a). From this observation, it can be inferred that the thickness of the wetted solder will be about 30 μm if all of the spacer is placed between the upper and bottom PCBs.

For a comparison of the electrical resistance between the smart ACA and a conventional ACF, both materials were used for a flip-chip bonding process with the same PCBs, and their electrical resistances were measured using 13 channels. The average electrical resistances are 4.88 mΩ with a small tolerance for the smart ACA and 36.29 mΩ with a large tolerance for the conventional ACF, as shown in Fig. 16. The electrical resistance by the wetted solder of the smart ACA is 7 times lower than that by the mechanical contact of the conventional ACF. Figure 17 shows the shear strength of the smart ACA after a pressure cook test (PCT). The PCT experiment was performed under the following conditions: 100°C temperature, 1.0 atmospheric pressure, and 100%

relative humidity for 240 hrs. Before and after the PCT, the shear strengths were 506 kgf/cm^2 and 203 kgf/cm^2, respectively. After the PCT experiment, it is inferred that the adhesion strength is only carried by the wetted solder because 240 hours is long enough to exhaust the adhesion strength of the polymer material due to the water uptake. If the conventional ACF is exposed to the same PCT conditions, its adhesion of the polymer material will almost disappear.

IV. Conclusion

As a third-generation material for an electrical interconnection, a smart ACA material with the functions of electrical conduction and good adhesion strength was developed. For the optimum processing conditions and good electrical and mechanical performances after processing, a thermal analysis and characterization were conducted. Based on the experimental results, such as the optimum volume concentration of the spacer and applied pressure and temperature, the processing cycle and bonding mechanism with fluxing effect were carefully designed from a chemorheological view point. With the application of the smart ACA, SMT and an underfill process were unified. The use of the spacer with a polymer ball makes it easy to control the gap between both substrates. It is proved that the electrical and mechanical performances of the smart ACA is obviously superior to a conventional ACF.

Acknowledgements

The authors would thank S.W. Oh and K.J. Sung for supporting the sample preparation.

References

[1] J.H. Lau, *FlipChip Technologies*, New York: McGraw-Hill, 1995, pp. 123-179.

[2] M.L. Minges, *Electronic Materials Handbook: Packaging*, ASM International, 1989.

[3] W.S. Kwon and K.W. Park, "Contraction Stress Build-Up of Anisotropic Conductive Film (ACFs) for Flip-Chip Interconnection: Effect of Thermal and Mechanical Properties of ACFs," *J. Applied Polymer Science*, vol. 93, no. 6, 2004, pp. 2634-2641.

[4] J.W. Kim, W.C. Moon, and S.B. Jung, "Effects of Bonding Pressure on the Thermo-Mechanical Reliability of ACF Interconnection," *Microelectron. Eng.*, vol. 83, 2006, pp. 2335-2340.

[5] T. Sagawa et al., "Anisotropic Conductive Paste (ACP) Connection Technology," *Fujikura Technical Rev.*, 2005, pp. 33-37.

[6] J. Kivilahti and P. Savolainen, "Anisotropic Adhesives for Flip-Chip Bonding," *J. Electron. Manuf.*, vol. 5, no. 4, 1995, pp. 245-252.

[7] P. Savolainen and J. Kivilahti, "Electrical Properties of Solder Filled Anisotropically Conductive Adhesives," *J. Electron. Manuf.*, vol. 5, no. 1, 1995, pp. 19-26.

[8] J.M. Kim, K. Yasuda, and K. Fujimoto, "Isotropic Conductive Adhesive with Fusible Filler Particles," *J. Electron. Mater.*, vol. 33, no. 11, 2004, pp. 1331-1337.

[9] J.M. Kim, K. Yasuda, and K. Fujimoto, "Novel Interconnection Method Using Electrically Conductive Paste with Fusible Filler," *J. Electron. Mater.*, vol. 34, no. 5, 2005, pp. 600-604.

[10] C. Kallmayer et al., "Study Reflowable Underfill Materials for Different Flip Chip Processes," *ECTC*, 2000.

[11] S. Shi et al., "Study of the Fluxing Agent Effects on the Properties of No-Flow Underfill Materials for Flip-Chip Applications," *ECTC*, 1998.

[12] T. Wang et al., "Studies on a Reflowable Underfill for Flip Chip Application," *ECTC*, 2000.

[13] Y.S. Eom et al., "Characterization of Polymer Matrix and Low Melting Point Solder for Anisotropic Conductive Film," *Microelectron. Eng.*, vol. 85, 2008, pp. 327-331.

[14] Y.S. Eom et al., "Electrical and Mechanical Characterization of an Anisotropic Conductive Adhesive with a Low Melting Point Solder," *Microelectron. Eng.*, vol. 85, 2008, pp. 2202-2206.

[15] A. Hale, C.W. Macosko, and H.E. Bair, "Glass Transition Temperature as a Function of Conversion in Thermosetting Polymers," *Macromolecules*, vol. 24, 1991, pp. 2610-2621.

Yong-Sung Eom received his BS degree from Korea Aerospace University and his MS degree from Korea Advanced Institute of Science and Technology (KAIST), Seoul, Korea, in 1988 and 1991, respectively. From 1991 to 1995, he worked at the Korea Institute of Aeronautical Technology (KIAT) at Korean Air Ltd. as a design and process engineer for composite materials of the MD-11 Aircraft Spoiler. In 1999, he received his PhD degree from the Department of Material Science Engineering at Ecole Polytechnique Federale de Lausanne (EPFL), Lausanne, Switzerland. From 2000 to 2001, he worked as a packaging engineer for the memory device at Hynix Semiconductor Ltd. Since 2001, he has been with ETRI, Korea, where he has been working as a packaging engineer. His research activities include the characterization of polymer material for electronic packaging, process design for MEMS, and electronics device packaging.

Keon-Soo Jang received the MS degree from Sungkyunkwan University in Korea and is working at Korea Institute of Science and Technology (KIST), researching into intraocular lens (IOLs) based on a radical polymerization of P(MMA-co-HEMA). His primary research interest is in polymers, specifically focusing on conducting polymers and epoxy.

Jong-Tae Moon received the MS and PhD degrees in materials science from Hongik University, Seoul, South Korea, in 1990 and 1995, respectively. During 1996 to 1997, he joined the optical module package team at ETRI. During 1998 to 2000, he worked as the team manager in the advanced package team and developed the CSP package and wafer-level package for memory devices at Hyundai Electronics. Since 2001, he has researched the optical module package for low cost FTTH triplexer module in ETRI. His research interests are wafer-level MEMS packaging and electronic packaging material.

Jae-Do Nam is currently a professor at the Department of Polymer Science and Engineering, and an adjunct professor in the Department of Energy in Sungkyunkwan University, Suwon, Korea. He received the BS and MS in chemical engineering from Seoul National University, in 1984 and 1986, respectively. In 1991, he received the PhD in chemical engineering from the University of Washington, Seattle, WA, USA. He worked at the Polymeric Composites Laboratory, University of Washington, as a research associate from 1991 to 1993. Returning to Korea, he joined Jeil Synthetic Fiber Co., Samsung Group, from 1993 to 1994, and moved to Sungkyunkwan University in 1994. He has worked as a visiting professor in the Ecole Polytechnique Federale de Lausane (EPFL), Lausanne, Switzerland, supported by the Swiss Science Foundation. Currently, he is the Chairman of the Department of Polymer Science and Engineering, Sungkyunkwan University, the principal investigator of the Brain Pool 21st Century Program (Ministry of Education, Korea), and the director of "Eco-Friendly Sustainable Technology for Automobile" (Gyeonggi Province), Korea. He received a best-paper award from the Polymer Society of Korea, and was appointed as the best lecturer and distinguished researcher (2004~2009) in Sungkyunkwan University. He is actively working in the areas of thermoplastic/thermoset polymer nanocomposites, direct methanol fuel cell, electroactive actuators and sensors, polymer/metal/inorganic nanoparticle synthesis, self-assembly structuring, bodegradable nanocomposites, and micropackaging polymers/fabrication. He has authored or co-authored over 160 peer-reviewed articles and is named in more than 40 patents.